Supporting Information for "Metal-free, nitrogen-doped graphene used as a novel catalyst for dye-sensitized solar cell counter electrodes"

Ming-Yu Yen[a], *Chien-Kuo Hsieh*[b], *Chih-Chun Teng*[a], *Min-Chien Hsiao*[a], *Po-I Liu*[a], *and Chen-Chi M. Ma** [a], *Ming-Chi Tsai*[b], *Chuen-Horng Tsai*[b], *Yan-Ru Lin*[c], *and Tsung-Yu Chou*[d]

[a] Department of Chemical Engineering, National Tsing Hua University, Hsinchu 30013, Taiwan, R.O.C.

[b] Department of Engineering and System Science, National Tsing Hua University, Hsinchu 30013, Taiwan, R.O.C.

[c] Department of Materials Engineering, Ming-Chi University of Technology, Taipei, 24301, Taiwan, ROC

[d] Department of Mold and Die Engineering, National Kaohsiung University of Applied Sciences, Kaohsiung 807, Taiwan, R.O.C.

[*]Corresponding author.

Tel.: +886-35713058 Fax: +886-35715408

E-mail: ccma@che.nthu.edu.tw (Chen-Chi M. Ma)

1. Preparation and fabrication of electrodes of DSSCs

1.1. Preparation of GO, GR, and NGR.

The modified Hummers method[1] was used to oxidize graphite flakes (98% purity, -325 mesh, Alfar Aesar) to synthesize graphene oxide (GO). A total of 10 g graphite flakes were stirred for 7 days in a solution of 50 g potassium permanganate ($KMnO_4$) in concentrated H_2SO_4 and HNO_3 (the weight ratio of H_2SO_4 to HNO_3 was 4: 1), and were then reacted with H_2O_2 and washed with 5 wt. % aqueous hydrochloric acid solution to complete the oxidation and remove sulfate ions. The suspension was washed with deionized water and centrifuged repeatedly until the solution was neutral. The resulting brown powder was dried in a vacuum at room temperature to obtain GO. To compare the electrocatalytic properties of electrodes with those of NGR, we obtained graphene from a chemical reduction using sodium borohydride ($NaBH_4$). NGR composites were prepared using the hydrothermal method.[2]

1.2. Preparation of various counter electrodes and fabrication of DSSCs.

The paste containing graphene and NGR were fabricated as follows. First, 85 wt. % carbon materials, 10 wt. % Polyvinylidene fluoride (PVDF), and 5 wt. % XC-72 were dispersed in N-Methyl-2-pyrrolidone (NMP) by using an ultrasonic horn for 1 h, thereby producing the carbon paste. The counter electrode with carbon materials was fabricated using solvent-casting in a vacuum overnight at 80^{o}C. To prepare the DSSC photoanodes, a layer of paste was coated on fluorine-doped tin oxide glass (TEC-7, 7 Ω square^{-1}, Hartford Glass Co., USA) plates. The coated electrodes were heated in air at 500^{o}C for 30 min. The thickness and active cell area of the TiO_2 film were approximately 10 μm and 0.25 cm^2, respectively. Prior to the fabrication of the DSSCs, the working electrodes were sensitized by soaking them for 24 h in a 3×10^{-4} M solution of ruthenium dye (cis-dithiocyanato-N,N'-bis

(2,2'-bipyridyl-4-carboxylicacid- 4'-tetra-butylammonium carboxylate) ruthenium (II); N719, Solaronix SA, Switzerland) in acetonitrile / *t*-butyl alcohol (*v*:*v* = 1:1). The sensitized electrodes were then immersed in acetonitrile for 12 h. The DSSC comprised a sensitized working electrode, various counter electrodes, and an electrolyte with a 60-μm-thick hot-melt sealing foil (SX1170-60, Solaronix SA, Switzerland) between each layer. The electrolyte used in this study consisted of 0.6M 1-butyl-3-methylimidazolium iodide (BMII), 0.1M guanidinium thiocyanate, 0.03M iodine, and 0.5M 4-tert-butylpyridine (TBP) in acetonitrile / valeronitrile (volume ratio: 85:15)). A DSSC device composed of these materials is shown in Fig. S1.

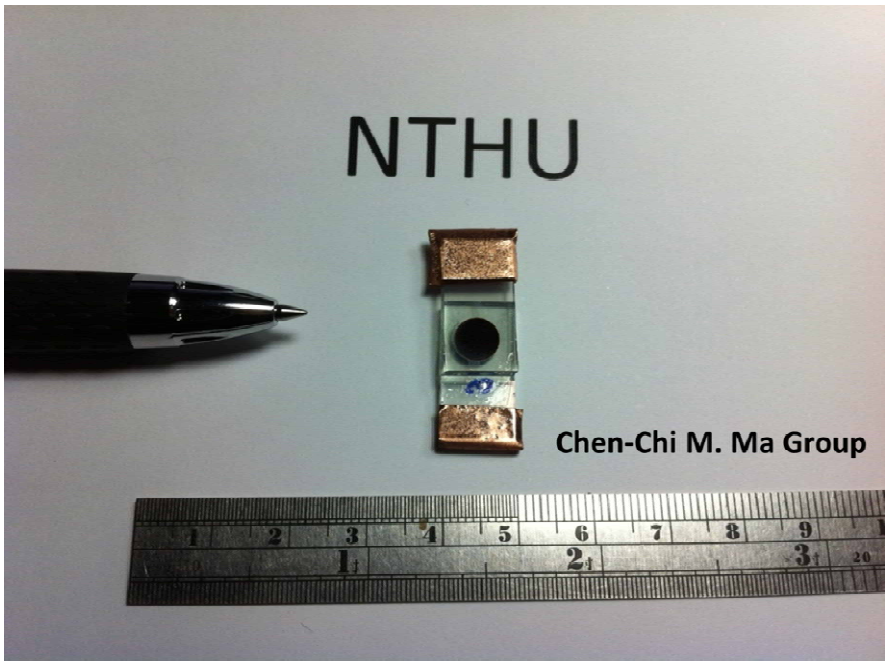

Figure S1. Photograph of our DSSC device comprising of NGR counter electrode.

1.3. Characterization of composite counter electrodes

X-ray diffraction (XRD) measurements were conducted at room temperature at a scan rate of 2◦ min^{-1} using a Shimadzu XD-5 X-ray diffractor (40 kV, 30 mA, λ=0.1542 nm) with a copper target and Ni filter. Thermogravimetric analysis (TGA)

was conducted using a DuPont-TGA951 with a heating rate of 2°C min^{-1} in air. X-ray photoelectron spectra (XPS) were obtained using a PHI Quantera SXM/AES 650 Auger Electron Spectrometer (ULVAC-PHI INC., Japan) equipped with a hemispherical electron analyzer and a scanning monochromated Al Kα ($h\upsilon$=1486.6 eV) X-ray source. A small spot lens system allowed the analysis of samples with an area of less than 1 mm^2. Raman spectra were recorded using a LabRam I confocal Raman spectrometer (Dilor, France). The excitation wavelength was 488 nm from an He-Ne laser with a laser power of approximately 15 mW at the surface of the sample. The morphology of the composite working electrodes was then studied using scanning electron microscopy (SEM, Hitachi S-4700I, Japan), and the microstructures of the carbon materials were also investigated using transmission electron microscopy (TEM, JEOL 2100F, Japan) at an accelerated voltage of 200 kV. Cyclic voltammetric measurements were conducted using a potentiostat/galvanostat (PGSTAT 302N, Autolab, EcoChemie, Netherlands) in a three electrode configuration. Pt wire and an Ag/AgCl electrode were used as the counter and reference electrodes, respectively. Electrochemical impedance spectra (EIS) were obtained using the previously mentioned potentiostat/galvanostat equipped with a Frequency Response Analysis (FRA) module. In the scan, the frequency ranged from 10^6 to 10^{-1} Hz at an applied voltage of 10 mV. Impedance spectra were analyzed using an equivalent circuit model with Autolab FRA software (v4.9, Eco Chemie B.V.). The photocurrent–voltage characteristics of the electrodes were measured using a 2400 digital source meter (Keithley, USA) under illumination by a Class A sunlight simulator of 100 mW cm^{-2} (91160A, AM 1.5, Oriel, Newport Corporation, USA), which was equipped with an AM 1.5G filter (81088A, Oriel, Newport Corporation, USA) and a 300 W xenon lamp (6258, Oriel, Newport Corporation, USA). The intensity of the simulated incident

light was calibrated up to 100 mW cm^{-2} using a reference Si solar cell, which was calibrated at NREL (USA).

2. XRD patterns for graphene oxide, graphene, and nitrogen-doped graphene

Fig. S2 shows XRD patterns for graphene oxide (GO), graphene (GR), and nitrogen-doped graphene (NGR). The graphite showed a significant (002) peak at 26.3°, and a d-spacing of 0.34 nm.[4] As the graphite was oxidized to GO, the (002) graphite peak shifted to a lower angle of 10.68 °, with a d-spacing of 0.83 nm. The large interlayer distance of the GO was attributed to the presence of hydroxyl, epoxy, and carboxyl groups. In the present study, the common reducing agent $NaBH_4$ was used to reduce GO to graphene. Following the reduction, the sharp (002) peak of GO disappeared; the (002) peak of graphene was observed at 24.2°, with an interlayer distance of 0.37 nm, indicating that the graphene removed some of the oxygen-contained functional groups. The XRD pattern for the NGR composite showed that the graphite structure was successfully reduced on the graphene, with an identical d-spacing of 0.37 nm. In addition, the composite peaks at $2\theta = 24.28°$ could be assigned to the (002) graphite structure, similar to the XRD results for the GR materials.

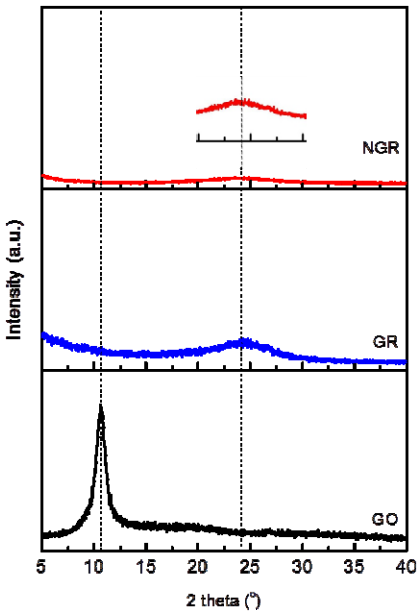

Figure S2. XRD patterns of GO, GR, and NGR

3. TEM, SEM, and AFM images of GO, GR, and NGR

The morphology of the carbonaceous materials was investigated using TEM and SEM to observe the differences between GO, GR, and NGR. Fig. S3(a) shows that the morphology of GO was characterized by an even surface with slight wrinkles, and an area with a dimension of 5.65 μm × 2.92 μm. Fig. S3(c) shows that following reduction by $NaBH_4$, the morphology of smaller dimensions was produced with a wrinkled rough surface; this was attributed to the stacking of several different pieces of graphene because of the effect of strong π-π stacking interaction on the graphene surface. The morphologies of the GR and NGR electrodes appeared to be similar at low magnification; however, high-magnification imaging revealed that they were entirely different (as shown in the manuscript). In addition, The TEM images of GR and NGR indicate that the thickness of those carbonaceous electrodes is similar to 4~6 layers (Fig. S4). Similar results were also observed in the measurements of AFM, as shown in Fig. S5. In addition, the R_a of GR and NGR was 11.21 nm and 23.95 nm, respectively.

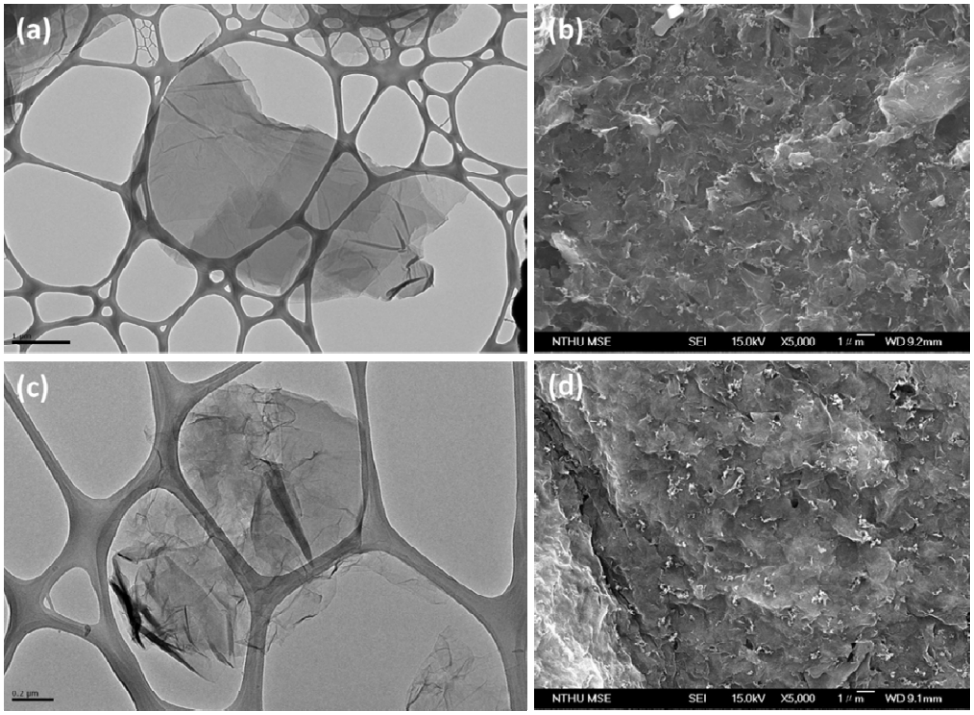

Figure S3. TEM images of (a) GO and (c) GR, and SEM images of the (b) GR and (d) NGR counter electrodes

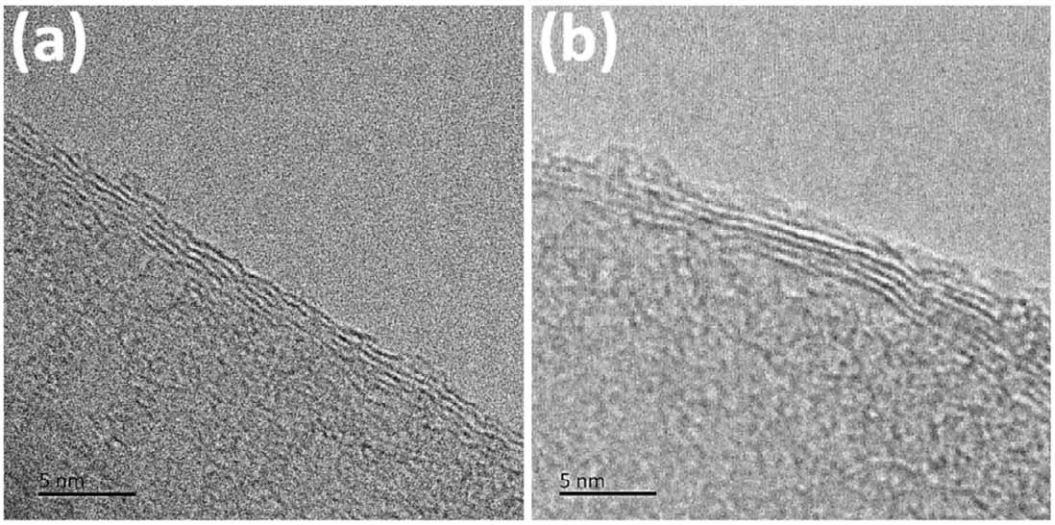

Figure S4. The TEM images of the thickness of (a) GR and (b) NGR carbon materials.

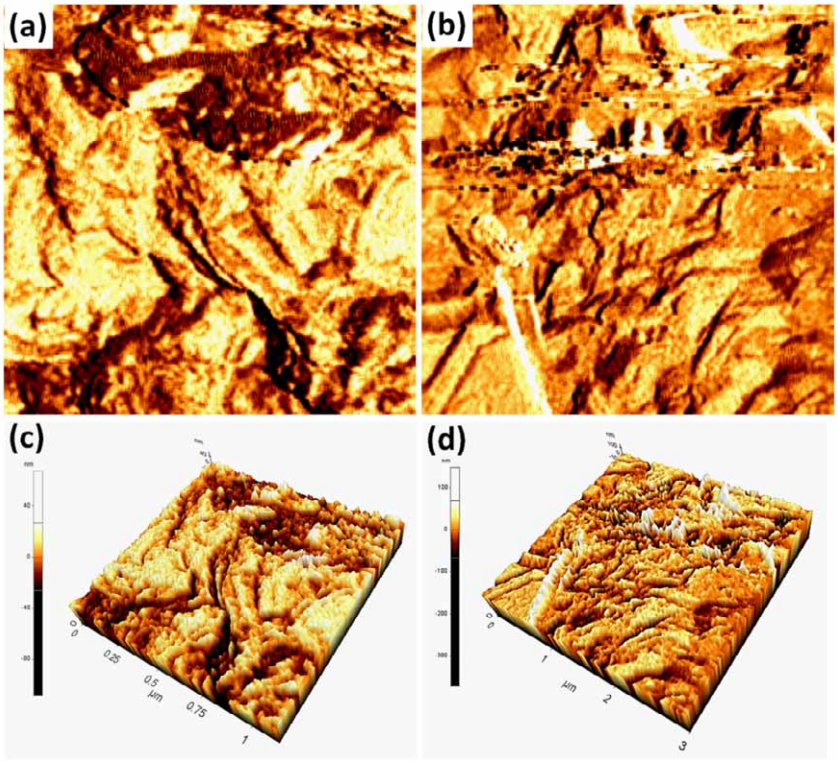

Figure S5 AFM images of (a) the surface of GR and (b) NGR electrode; 3D AFM images of (c) GR and (d) NGR.

4. Characterization of EIS spectra of GO, GR, and NGR

Table S1 Series resistance (R_s), charge transfer resistance (R_{ct}), and diffusion resistance (R_d) of DSSCs fabricated using various carbonaceous electrodes.

Electrode No.	R_s (Ωcm^2)	R_{ct} (Ωcm^2)	R_d (Ωcm^2)
Pt films	23.67	90.37	8.00
GR	24.25	6.31	3.82
NGR	24.02	1.30	0.016

5. Characterization of XPS spectra of GO, GR, and NGR

The C1s core level spectra of GO indicated a high degree of oxidation. Following reduction by $NaBH_4$, the GO was almost converted into GR, according to the changes in the C-O-C groups. The percentage of C=C groups increased because of the increased extent of the aromatic domains; this was illustrated by the appearance of the

π–π* satellite peak at 291.0 eV, which reflected the delocalization of the π–electrons in the aromatic network of the graphite.

Table S2. C1s peak positions, and atomic percentages of GO, GR, and NGR

samples	Fitting of the C1s peak binding energy (eV) (atomic percentage (%))						
	C=C (sp^2)	C-C (sp^3)	C-O	C-O-C	C=O	C(O)O	π-π*
GO	284.4 (11.51)	285.1 (25.60)	286.1 (43.44)	286.6 (7.30)	287.4 (8.37)	288.7 (3.78)	-
GR	284.4 (41.16)	285.0 (23.37)	285.9 (16.48)	286.9 (5.91)	287.8 (5.42)	289.3 (4.24)	291.0 (3.41)

samples	Fitting of the C1s peak binding energy (eV) (atomic percentage (%))				
	C=C (sp^2)	C-N		C(O)O	π-π*
NGR	284.7 (46.2)	285.6 (28.0)	287.0 (12.9)	289.1 (7.5)	291.0 (5.4)

6. References

1. W. S. Hummers and R. E. Offeman, *J. Am. Chem. Soc.*, 1958, **80**, 1339-1339.
2. D. Long, W. Li, L. Ling, J. Miyawaki, I. Mochida and S.-H. Yoon, *Langmuir*, 2010, **26**, 16096-16102.
3. S. Ito, T. N. Murakami, P. Comte, P. Liska, C. Grätzel, M. K. Nazeeruddin and M. Grätzel, *Thin Solid Films*, 2008, **516**, 4613-4619.
4. M.-C. Hsiao, S.-H. Liao, M.-Y. Yen, C.-C. Teng, S.-H. Lee, N.-W. Pu, C.-A. Wang, Y. Sung, M.-D. Ger, C.-C. M. Ma and M.-H. Hsiao, *J. Mater. Chem.*, 2010, **20**, 8496-8505.